

THE BEARING CAPACITY PARAMETER ANALYSIS AND HEAT ENERGY STORAGE LOSS TEST OF CONCRETE COMPOSITE BOX GIRDER

by

Baojia GONG^{a,b*}

^a College of Civil Engineering, Lanzhou Jiaotong University,
Anning District, Lanzhou, Gansu, China

^b Key Laboratory of Road and Bridge and Underground Engineering of Gansu Province,
Anning District, Lanzhou, Gansu, China

Original scientific paper
<https://doi.org/10.2298/TSCI2302207G>

In order to study the relationship between the bearing capacity of the structure and the damage degree, the author proposed the bearing capacity parameter analysis and the heat storage loss test of the concrete composite box girder. Taking the five-span prestressed concrete composite box girder as an example, different degrees of damage are simulated by reducing the bending stiffness of different parts, and the modal strain energy method and flexibility difference method are used to diagnose the structural damage. The test results show that for the first span, the sum of the structure can meet the corresponding specification requirements under the condition of dense traffic and less than 20% damage. When the damage is greater than 20%, the first span beam cannot meet the driving requirements. Under general traffic conditions, when the damage is less than 30%, the structure can basically meet the driving requirements, and the second and third spans still have a high safety factor. In the case of 30% damage of the first span, although β it does not meet the requirements, but $R_F > 0.9$. Each monitoring point has good estimation accuracy, and the error between the maximum temperature occurrence time of each monitoring point and the maximum temperature occurrence time of the monitoring point is within ± 10 hours. For continuous composite box girder structure, the flexibility difference method is superior to the modal strain energy method.

Key words: bridge engineering, composite box beam, injury diagnosis, the bearing capacity, reliability, heat loss

Introduction

In the past, reinforced concrete bridges, prestressed concrete bridges, dirty arch bridges and other structural forms were used. With the continuous improvement of road grade and the expansion of construction scale, bridges show the development trend of larger and larger span, richer and richer bridge type, and lighter and lighter structure, at the same time, more and more attention is paid to the economy of bridge construction. Given this background and demand, in many cases, the traditional bridge structure cannot meet the requirements of design, construction and use. The development of composite structure provides a new way to solve some technical problems in bridge engineering and becomes one of the important development directions of bridge structure system. In recent years, the application practice shows that the steel-concrete composite structure bridge is simple in construction and convenient in construc-

* Author's e-mail: baojiagong@126.com

tion, with simple construction technology, good structural performance can be obtained, it has the characteristics of *light and large span, prefabricated assembly, rapid construction*, and so on, it can produce high technical and economic benefits and social benefits, in line with the requirements of modern structure and the national conditions of the development of capital construction. Therefore, it has a wide application prospect in the field of bridge structure and is favored by construction units and construction units. Steel-concrete composite box girder is one of the most common structure forms of steel-concrete composite structure, it is a new structure form developed on the basis of steel structure, concrete structure and thin-walled box girder structure, it consists of an upper reinforced concrete slab (or prestressed concrete slab) and a lower steel box girder, which is connected by shear connectors. Compared with the reinforced concrete box girder, the composite box girder has the advantages of small component size, light dead weight, shock resistance, good durability, economic applicability and so on. During the construction, the structure can also support less or no die, making the construction convenient and fast. Compared with the steel structure, it can reduce the amount of steel, increase the stiffness, increase the stability, therefore, it is not only often used for curved bridges, but also easy to realize the long span of bridges. However, this combination form of steel roof fails to make full use of, so there is the combination form of trough section steel box beam and concrete bridge panel, after canceling the steel roof, this combination form can save materials, but the construction accuracy and control requirements are higher, fig. 1.

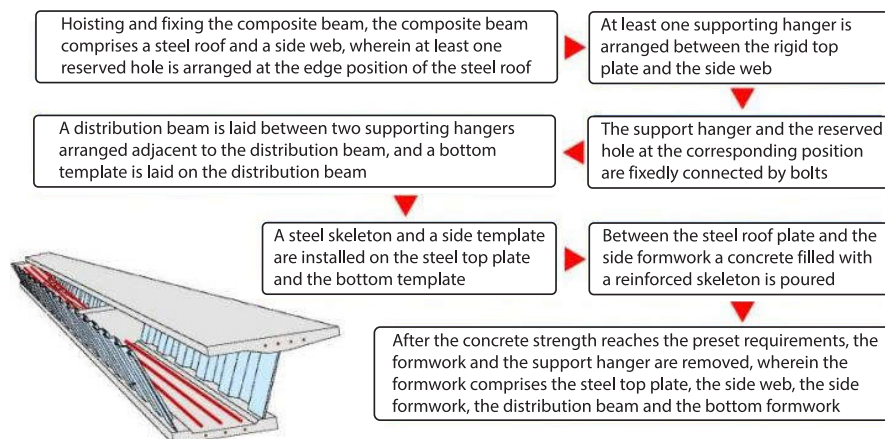


Figure 1. Analysis of bearing capacity parameters of concrete composite box girder

Literature review

The model test can intuitively reflect the whole process of the structure from the elastic working stage to the final ultimate failure stage, which can verify the correctness of the theoretical analysis and numerical analysis. At present, most of the model tests of shear lag research on box girders are made of concrete or plexiglas, and most of the external load forms mainly focus on symmetric concentrated load and uniform distributed load [1].

Lu *et al.* [2] made Plexiglas three-span continuous box girder bridge with variable height and cantilever beam model, and tested the deflection and strain values across the medium main section by using two loading forms, namely, concentrated load and distributed load, and verified their theoretical model. Shen *et al.* [3] made a large proportion of steel box girder test model, and carried out loading test research under the combination of concentrated load,

uniform load and other working conditions, the influences of the setting of the box girder diaphragm and the position of the external load in the transverse section on the shear lag effect of the box girder are further discussed, the variation law of shear hysteresis effect of simply supported steel box girder under various load forms is determined. Dong *et al.* [4] conducted 1:12 scale model test of steel-concrete composite box girder, and the elastic and plastic test results verified the variation rule of shear lag effect along the longitudinal direction of steel-concrete composite box girder, at the same time, the transverse position of the load has a great influence on the shear lag effect of the composite box girder, while the setting of the mid-span diaphragm has a small influence on the shear lag effect of the composite box girder. Jing [5] made a two-span model beam with corrugated steel webs of equal section, and the test results showed that, under the action of load, the composite continuous box girder has a phenomenon of shear lag, and the shear lag effect under concentrated load is significantly larger than that under uniformly distributed load. Nicoletti *et al.* [6], loading experimental research on the plexiglass indoor model of single-box, two-chamber and three-chamber simply supported box beams, compared with the deflection calculated by the material mechanics method, the deflection of double-chamber and three-chamber simply supported box beams is significantly increased after considering the shear lag effect.

Based on the actual project, the author takes the prestressed concrete composite box girder with five spans and one link as an example, and uses the modal strain energy method and the compliance difference method to identify the damage of the structure, on the basis of determining the degree of damage and its location, the relationship between the degree of damage and the bearing capacity of the structure is discussed. The thermal energy loss under different thin wall thicknesses is analyzed with the example of this project.

Research methods

Damage identification and localization method

According to the modal analysis theory, the compliance matrix of the lossless structure:

$$F = \sum_{i=1}^N \frac{1}{\omega_i^2} \Phi_i \Phi_i^T \quad (1)$$

where ω_i is the i^{th} mode frequency, N – the system order, and Φ_i – the i^{th} mode shape.

The compliance matrix of the damaged structure:

$$F^d = \sum_{i=1}^N \frac{1}{(\omega_i^d)^2} \Phi_i^d (\Phi_i^d)^T \quad (2)$$

where ω_i^d and Φ_i^d , respectively, represent the corresponding modal frequencies and modes after structural damage.

The difference matrix of structural compliance calculated by mode before and after structural damage is shown:

$$\Delta F = F^d - F \quad (3)$$

For the beam structure, if the flexural function of the beam is $w(x)$, then the total strain energy in the beam is expressed:

$$U = \frac{1}{2} \int_0^l E \left(\frac{\partial^2 w}{\partial x^2} \right)^2 dx \quad (4)$$

where E is the flexural stiffness of the section and x – the vertical position.

The j^{th} element corresponds to the element strain energy of the i^{th} mode:

$$U_{ij} = \frac{1}{4} E_j \left[\left(\Phi_{ij}'' \right)^2 + \left(\Phi_{i(j+1)}'' \right)^2 \right] (x_{j+1} - x_j) \quad (5)$$

Similarly, the element strain energy after damage can be obtained:

$$U_{ij}^d = \frac{1}{4} E_j \left[\left(\Phi_{ij}''^d \right)^2 + \left(\Phi_{i(j+1)}''^d \right)^2 \right] (x_{j+1} - x_j) \quad (6)$$

where Φ_{ij}'' , $\Phi_{i(j+1)}''$, $\Phi_{ij}''^d$, and $\Phi_{i(j+1)}''^d$ are the modes before and after damage, respectively, which can be obtained from the measured displacement modes.

In order to reduce the influence of random noise of test mode shapes, multi-order mode shapes are used to diagnose the damage position of the structure, as shown:

$$L_{\text{MSEC}_j} = \frac{1}{m} \sum_{i=1}^m L_{\text{MSEC}_{ij}} \quad (7)$$

where L_{MSEC_j} is the change of the average modal strain energy of m order mode of element j before and after structural failure, $L_{\text{MSEC}_{ij}}$ – the change of the i^{th} mode strain energy of element j before and after structural failure, $L_{\text{MSEC}_{ij}} = U_{ij}^d - U_{ij}$.

Example calculation

Taking a five-span structure of simply supported and then continuously partially prestressed concrete continuous box girder as an example, establish the finite element model. The superstructure of the main bridge is five holes, the single hole span is 30 m, the width of the bridge deck lane is 12 m, and the transverse structure is composed of four single box and single chamber box beams, which are connected through the cast-in-place transverse wet joints. Mid-span section box girder roof 180 mm, web 180 mm, and bottom 150 mm. Support section box girder roof 180 mm, web 250 mm, and bottom 250 mm. The structure is only provided with cast-in-place diaphragm at the support, and the lower part is a double column pier [7].

According to the stress characteristics of the structure, the side beam of the structure is in the most unfavorable stress state in the operation stage. Therefore, when damage simulation takes the middle span of the first straddle beam, the middle span of the second straddle beam and the middle span of the third straddle beam as the research object, under the condition of 10%, 20%, and 30% damage, respectively, modal strain energy method and compliance difference method are used to identify the structural damage, which is realized by reducing the element stiffness in the structural finite element model.

Result analysis

Structural bearing capacity analysis

JC method was proposed by Lachwitz and Fisley, Hashofer and Linde, *etc.*, it is suitable for solving the structural reliability index under arbitrary distribution of random variables, and the calculation accuracy meets the practical needs of engineering [8].

Dead load is a random variable generated by the dead weight of components that does not depend on the time parameter, it follows a normal distribution throughout its service. Based on the analysis of the measured traffic flow data, and considering the current highway live load classification and the convenience of subsequent calculation and analysis, the vehicle running state is divided into the general running state (highway II class) and the dense running state (highway I class). Since vehicle load is a random variable that depends on the time parameter,

therefore, it is considered that the probability distribution function of vehicle load effect follows the extreme value type I in the general operation state and the dense operation state. The statistical parameters of the effect are shown in tab. 1, where σ is the measured average value (standard value). For dead load, is the ratio of the measured dead weight of the structure to the designed dead weight of the structure. For live load, is the ratio of the effect value calculated by the measured vehicle load to the effect value calculated by the standard vehicle load specified in the current code. The δ is the coefficient of variation, tab. 1.

Table 1. Statistical parameters of effect

Type of action effect		Running state	σ	δ
Dead load	Component weight		0.9892	0.1115
	Bridge deck pavement		1.0213	0.0463
Live load (car) Intensive operation		Generally run	0.6962	0.1568
		0.7996	0.0862	

The bearing capacity coefficient of bridge structure stipulated in american bridge evaluation code:

$$R_F = \frac{C - \gamma_{D_C} D_C - \gamma_{D_W} D_W \pm \gamma_P P}{\gamma_L L (1 + I)} \quad (8)$$

where C is the strength limit state, $C = \varphi_c \varphi_s \varphi_R$, φ_c – the state coefficient, φ_s – the system coefficient, φ – the LRFD resistance coefficient, R – the nominal component resistance, D_C – the dead load effect caused by components and their accessories, D_W – the dead load effect caused by pavement, P – the permanent load except the dead load, L – the live load effect, I – the impact coefficient, and γ_{D_C} , γ_{D_W} , γ_P , and γ_L are the corresponding load coefficients of D_C , D_W , P , and L , respectively.

The main advantage of the American bridge evaluation code is that it is similar to the component coefficients in the design code, according to the statistical data and probability analysis, the reduction coefficients of the ultimate strength of materials, the load coefficients of dead load and live load are obtained, so the evaluation formula is relatively reasonable.

Equation (8) is used to calculate bridge R_F , where the parameter values are in accordance with the specification. Based on MATLAB software, the calculation program of R_F and reliability index β is developed, and the calculation results are shown in tab. 2 and 3.

According to tab. 2 and 3, the first span of the 5-span continuous beam structure has the most unfavorable force, followed by the third span, and the second span has the least force. Therefore, for the first span, under the condition of dense traffic and damage less than 20%, both R_F and β of the structure can meet the corresponding specification requirements. When the damage is greater than 20%, the first straddle beam cannot meet the driving requirements. The 20% damage of the first span structure can be regarded as the critical value of whether the bearing capacity meets the requirements:

- In general traffic conditions, the structure can basically meet the driving requirements within 30% damage, and the second and third spans still have a high safety factor. In the case of 30% damage of the first span, although β does not meet the requirements, $R_F > 0.9$.
- Under any traffic condition and the same location and degree of structural damage, β and R_F can basically indicate whether the structure meets the use requirements.

Table 2. Parameters under dense traffic conditions

Unit	The degree of damage [%]	R_F	β
The first straddle beam is in the middle of the span	10	1.0482	5.0101
	20	0.8625	4.3025
	0	0.6769	3.5376
The second straddle beam is in the middle of the span	10	1.5771	6.4034
	20	1.3794	5.7838
	30	1.1816	5.0605
The third side beam is in the middle of the span	10	1.3869	6.1259
	20	1.1982	5.4892
	30	1.0095	4.7503

Table 3. Parameters under general traffic conditions

Unit	The degree of damage [%]	R_F	β
The first straddle beam is in the middle of the span	10	1.3975	5.4464
	20	1.1500	4.7252
	0	0.9025	3.9392
The second straddle beam is in the middle of the span	10	2.1448	6.8570
	20	1.8759	6.2480
	30	1.6069	5.5400
The third side beam is in the middle of the span	10	1.8861	6.5841
	20	1.6295	5.9612
	30	1.3728	5.2301

Error analysis of hydrothermal estimation

In order to determine the error of hydrothermal estimation of hydraulic concrete, six temperature detection points are installed on the reinforcement site, the errors between the monitored values and the estimated values of the maximum temperature and occurrence time of water-heat exchange of hydraulic concrete are compared and analyzed, the statistical results of errors are shown in tab. 4 and fig. 2.

Table 4. Statistical results of maximum temperature and occurrence time error of hydraulic concrete

Serial number	T_{\max} [°C]			t [hour]		
	T_j	T_n	ΔT	t_j	t_n	Δt
1	43.11	44.03	-0.92	18.8	21.9	-3.1
2	45.52	45.76	-0.23	26.1	28.2	-2.1
3	53.57	53.42	0.14	30.3	37.6	-7.3
4	55.93	55.14	0.82	36.6	49.1	-12.5
5	57.16	57.60	-0.46	43.9	51.2	-7.3
6	64.12	65.59	-1.46	55.4	65.8	-10.5

In tab. 4 T_{\max} is the highest temperature, T_j – the highest temperature monitored value, T_n – the maximum temperature hydrothermal estimation value, ΔT – the error of the maximum temperature hydrothermal estimation and monitoring value at each monitoring point, t – the occurrence time of the highest temperature, t_j – the time when the highest temperature appears at the hydrothermal monitoring point, t_n – the occurrence time of the highest temperature of

the estimated hydrothermal value, and Δt – the error of estimating the maximum temperature occurrence time of each monitored water thermogenesis and the maximum temperature occurrence time of the monitoring point.

The error between the estimated value of maximum temperature hydrothermal at each monitoring point and the monitored value is lower than ± 1.5 °C, which has a good estimation accuracy, in addition, it can be seen from the estimation time of different maximum temperatures, the error between the occurrence time of the maximum temperature of each monitoring point and the occurrence time of the maximum temperature of each monitoring point is within ± 10 hours, which can basically meet the

requirements of the accuracy of the hydrothermal estimation in the construction code for hydraulic concrete (SL677-2014). For the maximum hydrothermal temperature of hydraulic concrete, it is mainly affected by the pouring time of hydraulic concrete and the thickness of thin wall, the temperature change of the hydrothermal temperature monitoring point is relatively slow, and the maximum temperature occurrence time is obviously later than that of other monitoring points. With the continuous increase of temperature, the estimation error of hydrothermalization is also increased, which is mainly due to the effect that the heat release temperature of hydraulic concrete has delayed change compared with its temperature increasing, which increases the calculation error [9].

Estimation of thermal energy loss under different thin-wall thicknesses

The thermal energy loss under different thin-wall thicknesses (40-150 cm) is estimated by using the hydrothermal estimation equation, the estimated heat loss rate of hydraulic concrete under different thin-wall thicknesses shows that, the temperature loss rate in the heat release process of hydraulic concrete generally shows a linear increasing change, and the highest value of heat loss rate mainly appears when the thin wall thickness is 120-140 cm, when the thickness of the thin wall reaches 150 cm, influenced by the peak temperature difference between internal and external heat release of hydraulic concrete, the increase of thermal energy loss rate has slowed down. With the increasing of thermal energy loss rate of hydraulic concrete, the surface temperature of hydraulic concrete changes greatly, which is mainly reflected in the obvious influence of temperature difference between inside and outside of the surface concrete. The thermal energy loss of surface hydraulic concrete reduces the temperature difference between inside and outside of surface hydraulic concrete under the thickness of 40-60 cm, and thus increases its temperature diffusivity [10].

Conclusion

Due to overload, environmental effects and functional degradation, highway bridges will lead to various structural damage. Therefore, while maintaining normal traffic conditions, how to accurately evaluate the residual capacity of existing highway bridges with damage has become an important problem to ensure the safety and smooth of highway traffic lines. Based on the actual project, the author takes five spans and one prestressed concrete composite box

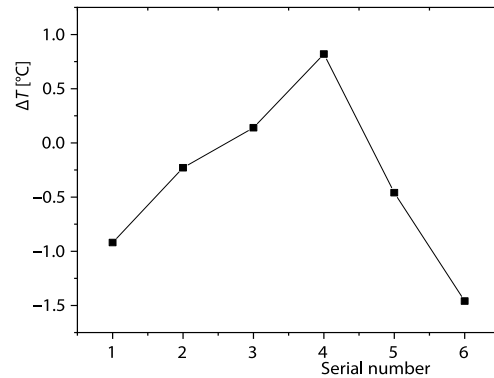


Figure 2. Error of estimated value and monitored value of maximum temperature hydrothermal of hydraulic concrete

girder as an example, modal strain energy method and compliance difference method are used to identify the damage of the structure, on the basis of determining the damage degree and location of the structure, the relationship between the damage degree and the bearing capacity of the structure is discussed, and the thermal energy loss is analyzed. Get the results: Under any traffic condition and with the same location and degree of structural damage, β and R_F can basically indicate whether the structure meets the use requirements. With the continuous increase of temperature, the error of hydrothermal estimation of different thin-wall thicknesses also increases, which is mainly affected by the delay of the heat release temperature of hydraulic concrete compared with its temperature increase, which increases the calculation error. Under the influence of temperature difference between inside and outside, the thermal energy loss rate of surface water of hydraulic concrete decreases obviously. Therefore, when the hydraulic concrete is poured, the temperature difference between inside and outside of the surface layer of hydraulic concrete should be reduced under the thin wall thickness of 40-60 cm, so as to improve its temperature diffusivity.

Acknowledgment

The authors would like to gratefully acknowledge the financial support from the National Natural Science Foundation of China. (Project No. 51568036 and No. 51868040).

Reference

- [1] Wang, H., *et al.*, Static Behavior of a Steel-Ultra High Performance Concrete Continuous Composite Box Girder, *Structure and Infrastructure Engineering*, 18 (2022), 8, pp. 1120-1137
- [2] Lu, P., *et al.*, Parameter and Sensitivity Reliability Analysis of Curved Composite Box Beam, *Mechanics Based Design of Structures and Machines*, 56 (2021), 2, pp. 1-18
- [3] Shen, D., *et al.*, Behavior of a 60-Year-Old Reinforced Concrete Box Beam Strengthened with Basalt Fiber-Reinforced Polymers Using Steel Plate Anchorage, *Journal of Advanced Concrete Technology*, 19 (2021), 11, pp. 1100-1119
- [4] Dong, J., *et al.*, Research on Flexural Behavior of Composite Box Continuous Girder with Corrugated Steel Webs and Trusses, *Advances in Structural Engineering*, 24 (2021), 15, pp. 3580-3593
- [5] Jing, Q., Continuous Steel Box Girders and Reinforced Concrete Structures in the Main Bridge Project of Hong Kong-Zhuhai-Macao Bridge, *Journal of Zhejiang University – Science A*, 21 (2020), 4, pp. 249-254
- [6] Nicoletti, R. S., *et al.*, Numerical Assessment of Effective width in Steel-Concrete Composite Box Girder Bridges, *Advances in Structural Engineering*, 24 (2021), 5, pp. 977-994
- [7] Lin, J. P., *et al.*, Analysis of Shear Connector of Steel – Concrete Composite Box-Girder Bridge Considering Interfacial Bonding and Friction, *International Journal of Steel Structures*, 20 (2020), 2, pp. 452-463
- [8] Zhang, X., *et al.*, An Experimental Study on the Flexural Behavior of Local Prestressed Steel-Concrete Composite Continuous Box Beams, *Advances in Structural Engineering*, 24 (2021), 2, pp. 307-319
- [9] Chaudhari, S. C., Deshmukh, S. K., Distortional Response of Doubly Symmetric Laminated Composite Box Girder, *Materials Today: Proceedings*, 27 (2020), 1, pp. 1381-1388
- [10] Xu, B., *et al.*, Fuzzy Comprehensive Evaluation Method for Integral Stability of Box G Girder with Corrugated Steel Webs, *Journal of Computational Methods in Sciences and Engineering, (Preprint)*, 23 (2021), 2, pp. 1-14